Anisotropy of diffusion along steps on the (111) faces of gold and silver

R. Ferrando* and G. Tréglia
Centre de Recherche sur les Mécanismes de la Croissance Cristalline, Centre National de la Recherche Scientifique, Campus de Luminy, Case 913, 13288 Marseille CEDEX 9, France
(Received 11 May 1994)

We present a molecular-dynamics simulation of adatom diffusion along the two close-packed steps on the (111) surfaces of gold and silver. Both metals are modeled by employing many-body potentials derived within the second-moment approximation to the tight-binding model. The simulation predicts very different behaviors for the two metals. For Au, the diffusion is much faster along the step with (111) microfacets (step B), whereas for Ag the diffusion is faster along the step with (100) microfacets (step A). The difference between the diffusion coefficients along the steps is more marked in gold and, for both metals, the Arrhenius plots show a dynamical lowering of the activation barriers with respect to the static potential barriers; no evidence of an inversion of the anisotropy of diffusion is obtained. As the diffusion along steps is quasi-one-dimensional, the results of the simulations have been compared to those based on the Fokker-Planck equation in a one-dimensional periodic potential. The agreement between the model and the simulations is remarkable for B steps both in gold and silver; the model predicts the temperature dependence of the rate, the correct proportion of long jumps, and the details of the behavior of the mean-square displacement. In A steps, the agreement is satisfactory for Ag and qualitative for Au; in the latter case, the diffusion path is rather different from a straight line and the application of a one-dimensional model may be questionable.

I. INTRODUCTION

The diffusion of adsorbed atoms on crystal surfaces is a topic of great interest from both the experimental and the theoretical point of views[1–6] since it plays a fundamental role in many surface processes, such as surface reactions, adsorption, desorption, and crystal and thin film growth. The diffusion of single adatoms on flat surfaces has been widely studied by experiments and simulations. It has been shown that adatoms may diffuse by different mechanisms, such as single jumps, long jumps,[7–12] and exchanges.[13–16]

Recently, the mobility of adatoms on stepped surfaces and on islands has attracted much interest, as it is fundamental for the understanding of growth mechanisms. For instance, the problems of step-edge descent on the (111) face of fcc metals and of the kinetics of deposition on top of the islands have stimulated much theoretical and experimental work.[17–21] On the contrary, much less is known about the diffusion along step edges. There are some results about the static barriers (at zero temperature) for diffusion along the close-packed steps on the (111) faces of silver[22] and aluminum,[18] but complete studies at zero and high temperature are still lacking. The diffusion along island edges is the dominant mass-transport mechanism in the two-dimensional spinodal decomposition of a half monolayer of Cu deposited on Cu(100).[23] Moreover, the anisotropy of diffusion along the close-packed steps on the (111) face of Pt may give an explanation of the temperature dependence of the growth shapes of two-dimensional islands.[24]

In this work we perform molecular-dynamics (MD) simulations of diffusion along the two kinds of close-packed steps on the (111) face of fcc transition metals, in particular of gold and silver. The two steps are shown in Fig. 1; step A has (100) microfacets on the step riser, whereas step B presents (111) microfacets. We have chosen gold and silver mainly because these metals represent two typical cases with opposite characteristics. In fact, as we will see in the following, the static barrier (zero temperature) for diffusion along the steps is higher along A steps for gold and along B steps for silver. Therefore we expect that gold and silver will display a rather different behavior with respect to the anisotropy of diffusion at steps. Moreover, the two metals present rather low barriers for diffusion along both steps. At present, MD simulations can be performed, with a reasonable amount of computer time, at most on the time scale of nanoseconds. Therefore this technique allows the determination of diffusion coefficients D of at least 10^{-6} cm^2/s. For what concerns diffusion along the steps A and B, it turns out that for gold and silver these values of D are attained around 500 K, a temperature close to that of sputtering

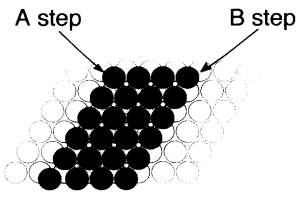

FIG. 1. A terrace on the (111) face of an fcc crystal, with an A step (square microfacets on the step riser) on the left and a B step (triangular microfacets on the step riser) on the right.

experiments on gold.[25] For simplicity, the simulation of gold has been done on the unreconstructed (111) surface. The periodicity of this reconstruction is very large[26] and therefore the simulation of the reconstructed surface at finite temperature is really cumbersome as it requires a very large simulation box. Moreover, due to the character itself of the reconstruction, we may expect that it is not very important for the local environment at a step.

To perform a realistic MD simulation of gold and silver we employ many-body potentials of the tight-binding type, as developed by Rosato, Guillopé, and Legrand (RGL).[27,28] These potentials provide a rather simple analytical formula for the forces among the atoms; for that reason it is possible to perform large-scale MD simulations, with thousands of atoms. The RGL potentials have been recently employed with good results in the study of diffusion of Ir, Cu, Rh, and Pt adatoms on the (100), (110), and (111) faces of the same metals[16] and of Ir dimers on the same Ir surfaces.[29]

The diffusion along straight steps is essentially one dimensional (1D) as the diffusing atom is tightly attached to the step. On the other hand, refined diffusion theories are better developed in the 1D case. Therefore a realistic MD simulation of diffusion along steps can be used to test the validity of the theory, with much more precision than the simulations of diffusion on the flat surface. In this paper, the results of the simulation will be compared to theoretical prediction given by the Fokker-Planck equation (FPE) in a 1D periodic potential. The use of the FPE and of similar approaches has a long tradition in the field of surface diffusion[4,30–36] with good results.

The paper is organized as follows. In Sec. II the RGL potentials are briefly described. In Sec. III the potential energy barriers for the different significant processes that may happen while an atom diffuses along a step are calculated. In Sec. IV the results of the MD simulation are shown and the comparison with those by the FPE is made. In Sec. V the conclusions are outlined.

II. MODEL

The many-body RGL potential has been developed on the basis of the second-moment approximation of the density of states in the tight-binding model.[27,37–40] In the RGL potential, the energy of an atom i is written as the sum of two terms. The first term is the band energy E_b^i;[38,39] this term has a many-body character and it models the effect of the local electronic density, which is important for describing the binding due to delocalized electrons:

$$E_b^i = -\left\{ \sum_{j,r_{ij}<r_c} \xi^2 \exp\left[-2q\left(\frac{r_{ij}}{r_0}-1\right)\right]\right\}^{1/2}. \quad (1)$$

ξ is an effective hopping integral, r_{ij} is the distance between the atoms i and j, r_c is the cut-off radius for the interaction, r_0 is the first-neighbor distance, and q describes the distance dependence of the hopping integral. The square root in Eq. (1) allows a correct description of surface relaxations and reconstructions,[40,41] which is not obtained by two-body potentials. The second term E_r^i is a pairwise repulsive interaction of the Born-Mayer type

$$E_r^i = \sum_{j,r_{ij}<r_c} A\exp\left[-p\left(\frac{r_{ij}}{r_0}-1\right)\right]. \quad (2)$$

The total energy is given by

$$E_c = \sum_i (E_b^i + E_r^i). \quad (3)$$

The four parameters (ξ, A, p, q) are fitted to the experimental values of the cohesive energy, the lattice parameter, the bulk modulus, and the elastic constants C_{44} and C' (for details see Appendix A in Ref. [27]). The cutoff r_c is taken as the second-neighbor distance and the potential is linked up to zero at the third-neighbor distance with a fifth-order polynomial in order to avoid discontinuities both in the energy and in the forces. The parameters values for gold and silver are given in Table I together with the values of the lattice spacing at zero temperature $a(0)$ $[a(0) = \sqrt{2}r_0]$. The values used here are different from those given in Ref. [26] because there r_c was taken to be equal to the nearest-neighbor distance.

Our system (see Fig. 2) is a (111) slab with a width of 9 layers in the z direction, perpendicular to the surface. On the surface plane, where periodic boundary conditions have been applied, the size is of 9 rows and 15 columns. The topmost layer of the slab consists of a smaller terrace of 7 columns, delimited by an A and a B step on the left- and on the right-hand side, respectively. Along each step there is a diffusing adatom. In the following when we will speak of an "adatom" we mean one of these atoms diffusing along a step, if not otherwise specified. The minimization of the energy at 0 K for a given structure has been obtained by a quenching procedure;[28] starting from the unrelaxed positions of the atoms, we solve the classical equations of motion;[42] the quenching procedure[43] consists in canceling the velocity of a particle whenever its product with the force acting on the particle is negative. This procedure allows a full relaxation. The quenching is terminated when the crystal reaches a temperature lower than 5×10^{-3} K. In order to calculate the energy at saddle points the unstable degrees of freedom of the system have to be fixed. For instance, in the case of the saddle-point energy for the diffusion of an adatom along a step, the coordinate to be fixed is the displacement of the adatom along the step itself; the other two coordinates of the adatom and all the degrees of freedom of the other atoms of the slab are allowed to relax.

TABLE I. Nearest-neighbor distance at 0 K and parameters of the potentials used in the MD simulations of gold and silver.

Metal	$a(0)$ (Å)	ξ (eV)	A (eV)	p	q
Au	4.07	1.855	0.2197	10.53	4.30
Ag	4.09	1.190	0.1031	10.85	3.18

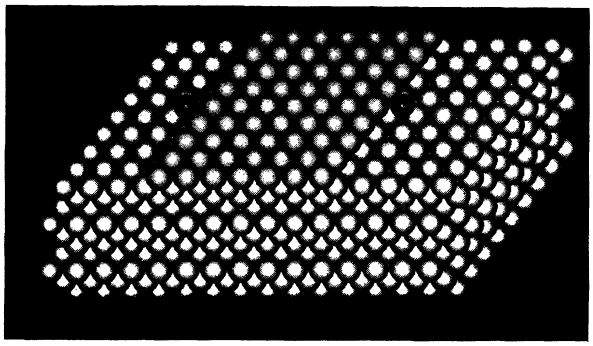

FIG. 2. The slab used in the simulations. The terrace on the topmost layer is bounded by an A step on the left and a B step on the right. In both channels along the steps there is an adatom.

The MD simulation at finite temperature is done in the microcanonical ensemble. The classical equations of motion are solved by the standard Verlet algorithm,[42] with a time step of 7×10^{-3} ps. Data are taken after a thermalization of 3000 steps, corresponding to 21 ps, which are sufficient to achieve equilibration. After that the simulation is performed for a considerable number of steps, of the order of 10^5. A typical length for our simulations is 560 ps. At each temperature considered, eight to ten simulations are done, in order to have a large number of events (essentially of jumps along the steps).

Our simulations have been performed in a rather wide range of temperatures, from 450 to 650 K. These temperatures are of the order of one-half of the melting temperatures of gold and silver and therefore thermal dilation must be taken into account. We have determined the thermal dilation at each temperature, looking for the value of the lattice parameter which corresponds to zero crystal pressure. To a high degree of accuracy, the thermal dilation is linear in that temperature range; the lattice parameter a increases with T according to the law

$$a(T) = a(0)\,[1 + \alpha(T - T_0)] \tag{4}$$

with $\alpha = 2.5 \times 10^{-5}$ K^{-1} and $T_0 = 88$ K for gold and $\alpha = 2.1 \times 10^{-5}$ K^{-1} and $T_0 = 81$ K for silver.

III. ENERGY BARRIERS AT 0 K

The motion of an adatom along a straight step is expected to be essentially 1D, as the adatom is tightly bound to the step itself, having five nearest neighbors instead of the three on the (111) flat surface. In both metals, the adatom in an equilibrium position along a step has an energy lower by about 0.4–0.5 eV than in an equilibrium position on the terrace. The minimum energy of an adatom in the channel along a step is essentially the same for the two steps in Ag and lower by 0.03 eV for step A in gold. Therefore the simple picture for the motion consists of jumps between the fcc equilibrium sites along the step. However, many different processes may happen; in principle, the adatom can exchange with an atom of the step, pushing the latter along the step or on the upper terrace; atoms of the step can come out and form a dimer with the adatom or diffuse along the step itself. Clearly, the importance of these different processes is determined by their time scales with respect to the time scale for the simple hopping. In order to clarify the relationships among these time scales, the energy barriers for the different elementary processes are computed by the quenching procedure sketched in the previous chapter.

The different elementary processes are shown in Fig. 3 (the figures show them for step A; the correspondence with the processes related to step B is trivial) and the numerical results are summarized in Table II. First of all we consider the simple hopping along the step [process (a) in the figures]. The barriers for gold are 0.340 and 0.224 eV for steps A and B, respectively. The corresponding barriers for silver are 0.254 and 0.289 eV. The values obtained for silver are in rather good agreement with those of embedded-atom calculations,[22] which are 0.207 eV for step A and 0.275 eV for step B. The barriers for hopping along the steps A and B are much larger than those for hopping on the flat surface both for gold and for silver. In fact, the barrier between an hcp site and a saddle point on the flat surface is 0.121 eV for Au and 0.067 eV for Ag [the embedded-atom result for silver is 0.060 eV (Ref. 22)]. For a single adatom, the fcc sites have a slightly higher energy, thus the barrier's fcc site saddle point are 0.116 and 0.058 eV, respectively. This is consistent with the results of field ion microscopy experiments,[44] which have shown that the hcp sites are favored for a single adatom of Ir on Ir(111). It should be noticed that a single jump along a step amounts to a double jump on the flat surface, because the hcp positions near the steps are not equilibrium sites. All the barriers for hopping along the two steps are of the order of 0.2–0.3 eV. However, the difference between the two barriers is considerable for gold (about 0.12 eV), but rather small (0.04 eV) and with the opposite sign for silver.

The diffusion paths along the two steps are rather different, as shown in Fig. 4. The path along step B is substantially a straight line, both in gold and in silver. The saddle-point positions are slightly displaced towards the step with respect to the minimum positions, by $\Delta y = -0.04$ and -0.01 Å for Au and Ag, respectively. In the z direction, the saddle point is at the same level as the minimum for silver and 0.03 Å higher for gold. Along this step the motion is really 1D. On the contrary, the path along step A shows pronounced deviations from a straight line. These deviations are not very important concerning the z coordinate (the saddle points are slightly below the minima, by $\Delta z = -0.10$ Å for gold and $\Delta z = -0.07$ Å for silver), but they are pronounced in the direction perpendicular to the step. The saddle points are displaced far away from the step, by $\Delta y = 0.71$ and 0.56 Å for Au and Ag, respectively. In the case of gold, the diffusion path is very close to the hcp position (see Fig. 4), which is displaced by $\Delta y = 0.83$ Å with respect to the minimum on the unrelaxed surface. The considerable barrier for diffusion in gold may be related to this large displacement of the diffusion path away from the step edge; however, the origin of the differences between gold and silver and their relationships with the

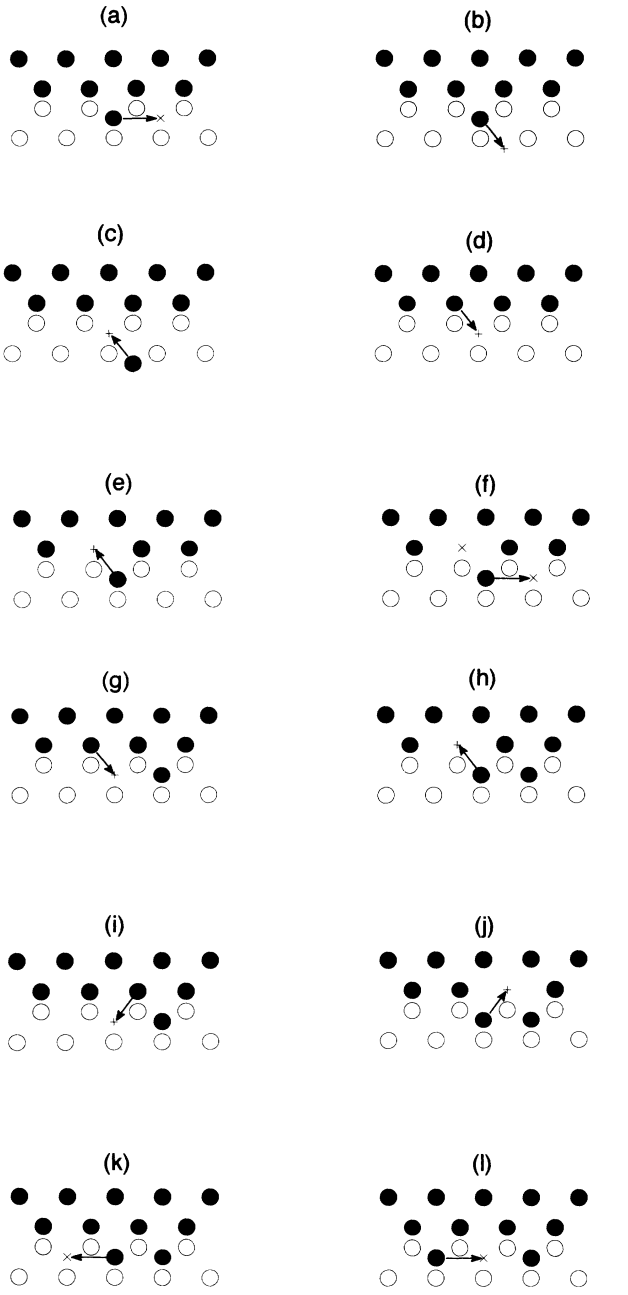

FIG. 3. Elementary processes (a)–(f) concern the diffusion of an adatom along a step and the disordering of the step. The processes are shown in the case of step A; the correspondence with those relating step B is trivial. In process (a) the adatom jumps along the step; in process (b) the adatom leaves the channel and reaches one of the nearest equilibrium sites on the terrace; process (c) is the reverse of (b); in (d) an atom of the step comes out in the channel; (e) is the reverse of (d); (f) follows (d) when the atom starts diffusing in the channel instead of coming back as in (e). Elementary processes (g)–(l) concern the formation and the dissociation of dimers along the step. In (g) an atom of the step comes out and a "stable" dimer (see text) in the channel is formed; (h) is the reverse of (g), i.e., the dimer is broken; in (i) an "unstable" dimer is formed; (j) is the reverse of (i); (k) and (l) show the dissociation and the formation of a third kind of dimer.

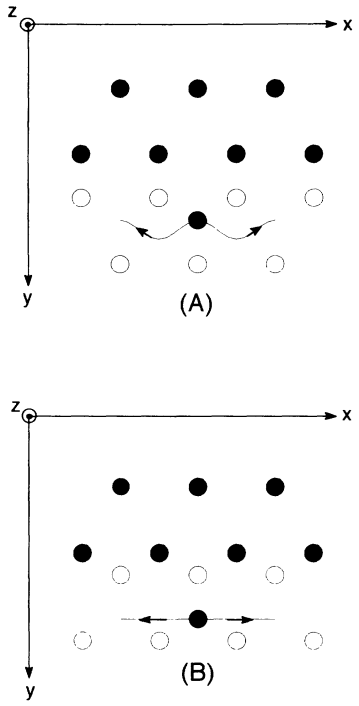

FIG. 4. Schematic representation of the diffusion paths along the two steps in the case of gold. In the case of silver the diffusion paths are similar, but the curvature of the path along step A is less pronounced.

potential parameters are currently under investigation.

We remark that all the displacements Δy and Δz refer to the fully relaxed crystal, after the quenching procedure. As the neighbors of the adatom are displaced from their positions with respect to a straight step, the "reference frame" for computing positions, and then displacements, is given by the step atoms far away from the adatom, because their positions are not perturbed by the presence of the adatom.

The adatom may leave the channel along the step to

TABLE II. Energy barriers related to the processes shown in Fig. 3. All the data are in eV.

Process	Au step A	Au step B	Ag step A	Ag step B
(a)	0.34	0.22	0.25	0.29
(b)	0.51	0.51	0.52	0.55
(c)	0.09	0.12	0.04	0.06
(d)	0.53	0.67	0.71	0.69
(e)	0.04	0.15	0.08	0.07
(f)	0.17	0.04	0.08	0.10
(g)	0.52	0.60	0.63	0.59
(h)	0.25	0.33	0.26	0.22
(i)	0.51	0.54	0.65	0.65
(j)	0.03	0.04	0.07	0.05
(k)	0.51	0.42	0.49	0.50
(l)	0.34	0.22	0.25	0.28

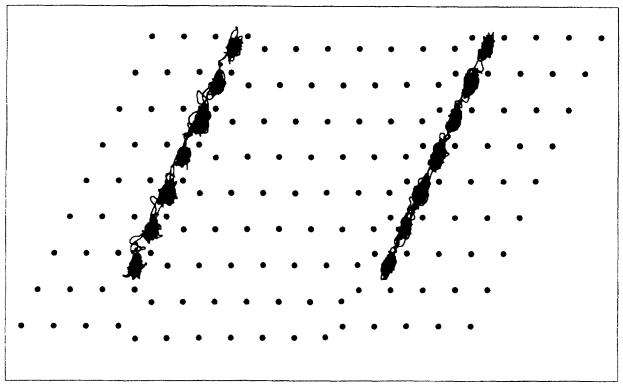

FIG. 5. Trajectories of the adatoms for a 560 ps simulation of Ag at 603 K. The trajectory along step A (on the left) shows that the saddle points are really displaced away from the step with respect to the minima.

reach one of the fcc equilibrium sites on the flat terrace as in process (b) in Fig. 3. In any case, two nearest-neighbor bonds must be broken in this process; therefore the barrier is rather high, around 0.5 eV (see Table II), for both steps in Au and Ag. The differences between the two metals are small and the departure from the step should be a rare event on the time scales of process (a) at any temperature of interest. Once the adatom has reached the fcc site it can diffuse on the terrace or come back and stick again to the step [process (c)]. In step A in both metals, the barrier for this process is slightly lower than the one for diffusion on the flat surface, by about 0.03 eV. An atom reaching the fcc site from step A has a definitely larger probability of coming back than of diffusing on the terrace up to temperatures around 400 K. This means also that an adatom diffusing on the lower terrace should be rather quickly trapped by the step, as the barrier for jumping into the channel is lower than that for diffusion on the flat terrace. This fact should lead to the depletion of adatoms on the lower terrace near a growing step, as it has been observed by field-ion microscopy around Ir clusters on Ir(111).[45] This is not the case in step B, as the barrier for coming back is the same as that for diffusion. Recently it has been found in different metals, such as Pt and Al,[46,18] that there is an energy gradient on lower terraces attracting adatoms towards steps. In our case we find that the potential acting on an adatom on the terrace is distorted by the presence of the step; however, the effect is important only in the vicinity of the step. For instance, we consider step A in silver. The energy of the system with the adatom in the channel along the step is 0.48 eV lower than the energy with the adatom on the lower terrace far away from the step; the *hcp* site near the step is not even an equilibrium site, being close to the saddle-point position for diffusion along the step. However, the energy of the adatom in the position taken at the end of process (b) is lower than that of the adatom far away from the step only by 0.01 eV. Therefore the effective attraction exerted on the adatom by the step seems to be rather short ranged.

Other possible processes are related to the displacements of atoms of the step which are far away from the adatom [processes (d)–(f)]. For instance, an atom of the step may leave the step itself to reach a metastable equilibrium position in the channel [process (d)]; from that position the atom may come back, as in (e), or diffuse along the step leaving a vacancy behind, as in (f) (we will not consider the back and forth motion between the two symmetric metastable sites on the two sides of the vacancy). Simple bond-counting predicts that the barrier for process (d) should be rather high, as the atom has to cut three nearest-neighbor bonds to reach the final position. This prediction is verified, but with some differences. The barriers for both steps in Ag and for step B in Au are of the order of 0.7 eV; these barriers are significantly higher than those for process (b), in which two bonds are broken. In step A in Au, the barrier is smaller, slightly above 0.5 eV and then process (d) might have a non-negligible frequency on the time scales of the simulation at finite temperature (see below). For instance, a rough estimate of the frequency of process (d) can be given by the transition state theory (TST);[47] according to TST the frequency of a process is given by $\nu \exp(-\Delta E/k_B T)$, where ν is a typical oscillation frequency and ΔE is the energy barrier. Assuming $\nu \sim 1$ ps^{-1} and taking $T \sim 600$ K, process (d) should happen on the scale of 10 ns for the step A of gold, of some 10^2 ns for step B, and on the scale of 1 μs for both steps in silver. If process (d) alone is considered, then the conclusion is that in gold step atoms will leave much more frequently step A to diffuse along the channel. However, this conclusion is not correct, because process (d) is not the whole history. From the metastable position in the channel, the atom is likely to come back [as in (e)] in the case of step A and to diffuse in the channel [as in (f)] in the case of step B. For step A at 600 K the probability of coming back is about ten times greater than the probability of starting diffusion in the channel; for step B, the ratio of the probabilities is inverted. This means that the difference in the barriers for process (d) is essentially compensated. In silver, there is no substantial difference between the steps; the very high barriers for process (d) and the good balance between the frequencies of events (e) and (f) should indicate that the kinetics of the disordering of straight steps is somewhat slower in Ag than in Au.

Another class of elementary processes that may take place when an adatom diffuses along a straight step is related to the formation and the dissociation of dimers. In the following we will consider the events concerning three different kinds of dimers, which are shown in Fig. 3.

The first two kinds, whose formation and dissociation are shown in (g),(h) and (i),(j), respectively, are formed because the step atoms in the vicinity of the adatom feel the attraction of the latter. In fact, the energy barriers for the formation of these dimers are lower than those for process (d), with differences of the order of 0.1 eV except for step A on gold, where the differences are negligible. Although the formation of the dimer of the first and the second kind involves the loss of two and three nearest-neighbor bonds, respectively, in all the cases the barrier

for process (g) is not very different from that for process (i), i.e., the differences are in any case much smaller than the strength of a bond and in the case of gold they are reversed. This is another example in which bond counting in the initial and final position can be misleading; the important thing for giving a picture of the kinetics of a process is the comparison between the initial and the saddle-point configurations. In fact, if we consider the atom coming out from the step in the saddle-point position, we can see that both in process (g) and in process (i) three nearest-neighbor bonds are broken; at the end of process (g) a new bond will be created with the adatom, but at the saddle point the distance is rather large and the attraction of the adatom may be rather small. The substantial difference between the two dimers is in their stability once they are formed, as results comparing the barriers for events (h) and (j). For instance, at 600 K, the stability of the second kind of dimer is always on the scale of few ps, while the first kind should survive on times of the order of 10^2 ps. As for the differences between step A and step B, Au and Ag behave (as usual) in the opposite way. In gold, dimers are formed easily on step A, but survival times are likely to be longer on step B; in silver the situation is reversed. As in previous cases, the anisotropy is more important in gold. Moreover, the formation of dimers is, on the average, faster in gold than in silver (especially for what concerns the dimer of the second kind) and dimers of the first kind are stabler in Au than in Ag. This is another indication of the fact that the kinetics of the disordering of straight steps should be faster in gold.

An important point related to the second kind of dimer concerns a possible exchange mechanism for diffusion. In fact, the situation represented in (j) is completely symmetric: the vacancy in the step can be filled either by the atom which has come out of the step or by the adatom which was in the channel at the beginning. In the latter case, the whole process [(i) and filling of the vacancy] amounts to a single jump of the adatom along the channel from the point of view of mass transport. If the exchange process can be modeled in this way, i.e., by a two-step process in which the atom of the step comes out and then the adatom fills the vacancy, its barrier should be essentially the one for process (i), which is the rate-limiting step. This implies that exchanges should be much more frequent in gold than in silver at any temperature of interest and even in gold they should take place on the scale of some ns at 600 K. However, the exchange process may take place by a concerted motion of the two atoms instead by the two-step mechanism creation of a vacancy-filling of the vacancy;[48] the barrier for a concerted motion may be lower,[49] as happens for exchanges on flat (100) and (110) surfaces. Process (j) may remind us of the migration of a vacancy on the flat surface. We remark, however, that process (j) presents much lower barriers than vacancy migration [0.31 eV in Ag Ref. 22], because in the latter case no bonds are gained.

The third kind of dimer is formed when two atoms meet each other on an otherwise straight step. The barriers for the formation [process (l)] do not differ from those for diffusion along the step [process (a)]. This is essentially due to the short-range character of the potential: the atom on the saddle point is too far away from the other atom in the channel to "feel" an appreciable attraction. Once the dimer is formed, its stability is considerable, the barriers for dissociation [process (k)] being at least of 0.4 eV. However, in gold, there is a marked difference between the two steps; at 600 K the time scale for the dissociation of the dimer along step A should be about five times longer than the one for the dimer along B (both time scales should be of the order of ns). Of course the ratio of these times increases at lower temperatures. In any case, the formation of such a dimer is a process hindering considerably the diffusion of both atoms.

Finally, we consider a process not shown in the figure, i.e., the exchange mechanism in which the adatom is incorporated in the step by pushing one atom of the step onto the upper terrace (this is the reverse process of the step descent by exchange). In gold, this process is characterized by a barrier of about 0.6 eV for both steps; in silver the barriers are somewhat higher, near 0.7 eV.

In conclusion, we remark that the times given in the above discussion are only indicative, first because our TST estimate is rough and second because the activation barriers at finite temperature (which are free-energy barriers) may be lower than the static energy barriers at 0 K.[33] The latter fact implies that the overall kinetics may be somewhat faster than indicated before. Therefore the ratios between the time scales are more important than the values given in the above discussion.

IV. MOLECULAR-DYNAMICS SIMULATION AT FINITE TEMPERATURE

A. Jump rate and diffusion coefficient

The comparison between the different time scales of the processes considered in the preceding section shows that an adatom put in the channel along a straight, close-packed step will perform, on the average, a rather large number of hoppings before the occurrence of events which lead to the disordering of the step or before the adatom itself will leave the step. This is of course true at low temperature, but it retains some validity even up to temperatures of the order of 600 K in both metals. In fact, at 600 K, the time scale for simple hopping varies from a maximum of some 10^2 ps for step A in gold to a minimum of some 10 ps for step B in gold while the characteristic times of processes (b), (d), (g), (i), and (k) in Fig. 3 are much longer. In a typical simulation on a time of the order of 500 ps only jumps of the adatoms (see Fig. 5) along the two close-packed steps occur. However, sometimes one of the different events described in Sec. III happens and the initial configuration consisting of only of one adatom along an otherwise straight step may change. As we are primarily interested in the diffusion of adatoms along straight steps, in each simulation and for both steps we have distinguished the total simulation time t_0 from the time t_1 in which only the adatom is in the channel along the step. If one or more other atoms

are in the channel, the motion of the adatom is considered perturbed by their presence. However, to give some indications about the kinetics of the disordering of the steps, we will keep record of all the different events which will take place.

The highest temperatures at which the simulations are performed are 592 K for gold and 635 K for silver. At these temperatures the ratios between the barriers for diffusion along the steps and thermal energy k_BT are in any case greater than 3 at least; therefore the adatoms are expected to spend the largest part of their time in small-amplitude oscillations in the vicinity of the equilibrium sites along the steps. In that case a jump-diffusion model can be safely applied;[50] the jump rate r_j and the mean-square jump length $\langle l^2 \rangle$ can be defined. The jump-diffusion model furnishes a simple estimate of the diffusion coefficient D in terms of r_j and $\langle l^2 \rangle$. In the case of a 1D motion the relation is

$$D = \frac{1}{2} r_j \langle l^2 \rangle. \tag{5}$$

Both r_j and $\langle l^2 \rangle$ can be easily extracted from the simulations by counting jumps and measuring their lengths. If only single jumps occur, $\langle l^2 \rangle$ is simply the square of the nearest-neighbor distance. However, in the field of surface diffusion, evidence of long jumps has been found in experiments[7–10,32,34] and MD simulations[11,12] and we expect that in our systems long jumps may play some role. In order to discriminate between single and long jumps in the simulations, some criterion is needed and we propose a simple one. For the explanation of this criterion it is better to start from examples of the typical trajectories of the adatoms during a simulation. Let us consider Figs. 5–7, where the results of a 560 ps simulation of silver at 603 K are shown. In Fig. 5 the trajectories of the two adatoms on the surface plane are plotted (step A and step B are on the left and on the right, respectively); in Figs. 6 and 7 the displacements in the direction along

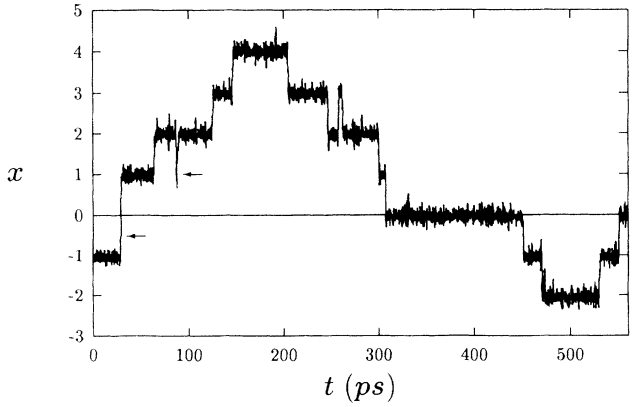

FIG. 6. Displacement x of the adatom along the step in a simulation of Ag at 603 K. The adatom spends long time periods by performing small oscillations around the equilibrium positions and sometimes makes sharp transitions from one cell to another. The arrows indicate a double jump at $t \simeq 30$ ps and an unsuccessful attempt (see text) at $t \simeq 90$ ps.

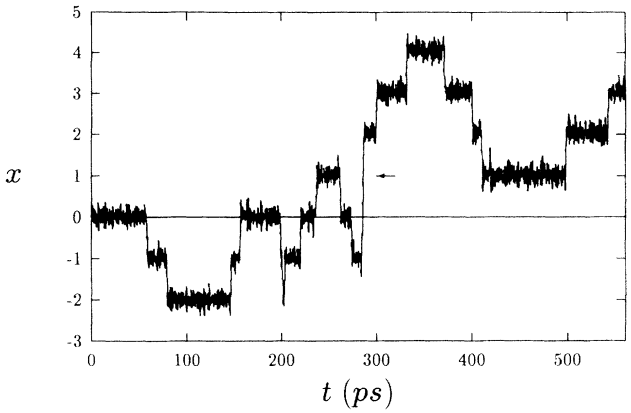

FIG. 7. As in Fig. 6, x displacement of the adatom along the step in a simulation of Ag at 603 K. The arrow indicates a triple jump.

the steps are given as functions of time. In this simulation the two adatoms diffuse by hopping in the channels and none of the other events described in Sec. III take place. The adatoms spend long time intervals by performing small oscillations at thermal equilibrium around the stable sites in the channels and sometimes they make sharply defined transitions from a cell to another. These transitions are rare events on the typical time scales of the oscillatory motion. This clearly shows that the diffusion along the channels can be modelized as a jump diffusion.[36] In order to map the jump-diffusion model on the continuous trajectories of the diffusing particles, we have to define the condition for considering a particle as thermalized in a given lattice cell. The natural condition can be expressed in terms of the time spent in that cell, which, at least, should be longer than the characteristic times of the intracell motion,[36,50] as the small-oscillation period $\tau_{\rm osc}$ and the thermal time $\tau_{\rm th}$, with

$$\tau_{\rm th} = a \left(\frac{m}{k_B T} \right)^{1/2}; \tag{6}$$

$\tau_{\rm th}$ is simply the time taken to cross the lattice spacing

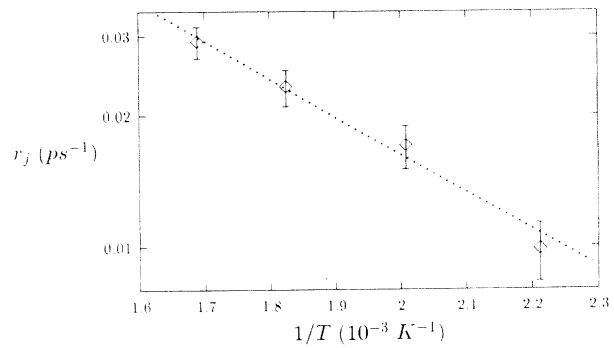

FIG. 8. Arrhenius plot of the jump rate r_j concerning diffusion along step B in Au. The error bars correspond to the standard deviation.

TABLE III. Results of the MD simulations of gold. T is the temperature, t_0 is the total simulation time, t_1 is the time in which only the adatom is in the channel along the step, r_j is the jump rate, and D is the diffusion coefficient.

Step	T (K)	t_0 (ps)	t_1 (ps)	Single jumps	Double jumps	r_j (ps^{-1})	D (cm^2 s^{-1})
A	452	4480	4480	2	0	$\sim 5 \times 10^{-4}$	$\sim 5 \times 10^{-7}$
A	498	4480	4409	5	0	$\sim 1 \times 10^{-3}$	$\sim 1 \times 10^{-6}$
A	548	5880	5868	27 + 1 exchange	0	0.5×10^{-2}	0.2×10^{-5}
A	592	5384	4961	38 + 2 exchanges	0	0.8×10^{-2}	0.3×10^{-5}
B	452	4480	4480	41	3	1.0×10^{-2}	0.5×10^{-5}
B	498	4480	4480	75	1	1.7×10^{-2}	0.8×10^{-5}
B	548	5880	5037	108	8	2.3×10^{-2}	1.2×10^{-5}
B	592	5384	5194	138	13	2.9×10^{-2}	1.6×10^{-5}

a by a particle with energy k_BT. In the case of jump diffusion, τ_{th} is larger than τ_{osc} (Ref. 36) and therefore the condition for the thermalization in a given cell can be expressed by requiring the diffusing particle to spend in the cell a time longer than τ_{th}. At 500 K τ_{th} amounts to 2 ps for gold and 1.5 ps for silver; in the following, these values are used in the practical application of the thermalization criterion.

From the thermalization criterion, the discrimination between different jump lengths follows. In fact, if two consecutive crossings of saddle points in the same direction are separated by less than τ_{th}, the particle is not thermalized in the cell in between and the event is computed as a double jump. If the two crossings are separated by a longer time, we have two distinct single jumps. Another case is that of a particle starting from a cell, crossing the saddle point, inverting its motion, and recrossing back. If the time between the crossing and the recrossing is less than τ_{th}, that event is considered as an unsuccessful attempt and not registered. If the time is larger, the event is computed as two distinct single jumps in opposite directions. As an example of the application of this criterion, we consider the trajectories of Figs. 6 and 7. In Fig. 6, besides many single jumps, there are a double jump and an unsuccessful attempt, both indicated by arrows. For the double jump the interval between the consecutive barrier crossings is 0.6 ps; for the unsuccessful trial it is 1 ps. In Fig. 7 a triple jump is indicated (a very rare event indeed), with intervals of 1.1 ps between the crossings of the first and of the second barrier and of 0.7 ps between those of the second and of the third. We remark that our method for discriminating long jumps is rather restrictive, as the thermalization criterion is essentially a necessary condition.

The results concerning the diffusion along the straight steps are summarized in Tables III and IV for Au and Ag, respectively. The occurrence of other events, such as formations of dimers and so on, will be discussed in the following. Only the exchanges originated by the formation of dimers of the second kind [process (i) in Fig. 3] are accounted for, as such an exchange is equivalent to a single jump from the point of view of mass transport. Of course, the exchanges are not taken into account in the determination of the jump rate, but only in that of the diffusion coefficient. When such exchanges occur, Eq. (5) may be modified as follows:

$$D = \frac{1}{2}(r_j + r_e)\langle l^2 \rangle, \tag{7}$$

where r_e is the exchange rate.

As results from both tables, the most common event is the single jump; double jumps occur along both steps in Ag and along step B in Au; the few exchanges are along step A in gold. The absence of long jumps along step A in Au may be related to two reasons. First of all, the diffusion barrier is high; the ratio of long jumps decreases with the dissipation in the lattice cell Δ,[51,36] which is proportional to the friction and to the square root of the barrier. Moreover, the diffusion path along this step is rather far from a straight line (see Fig. 5), which is usually the most favorable trajectory for long jumps, even in the case of two-dimensional diffusion.[11] Along the other steps, the proportion of long jumps never reaches 10%. The dependence with temperature of this

TABLE IV. Results of the MD simulations of silver. T is the temperature, t_0 is the total simulation time, t_1 is the time in which only the adatom is in the channel along the step, r_j is the jump rate, and D is the diffusion coefficient.

Step	T (K)	t_0 (ps)	t_1 (ps)	Single jumps	Double jumps	r_j (ps^{-1})	D (cm^2 s^{-1})
A	501	4480	4480	47	0	1.1×10^{-2}	0.5×10^{-5}
A	546	4480	4478	77	2	1.8×10^{-2}	0.8×10^{-5}
A	603	4250	4239	113	8	2.9×10^{-2}	1.4×10^{-5}
A	635	4480	4352	128	9	3.2×10^{-2}	1.6×10^{-5}
B	501	4480	4480	36	0	0.8×10^{-2}	0.3×10^{-5}
B	546	4480	4480	59	2	1.4×10^{-2}	0.6×10^{-5}
B	603	4250	4154	85	3 + 1 triple	2.1×10^{-2}	1.1×10^{-5}
B	635	4480	4397	104	8	2.6×10^{-2}	1.3×10^{-5}

proportion is not clear from our results, due to the rather poor statistics. For step B in Au, the percentage of long jumps does not seem to depend strongly on temperature, being of the order of 8% at $T = 452, 548$, and 592 K; the exception is $T = 498$ K, where only one double jump has been recorded. In silver, there is a clearer indication of some increase of the probability of long jumps with temperature, but with maximum percentages of 7%.

The exchanges are infrequent events; thus the statistics is poor (only 3). However, it is significant that all of them occur along the A step of Au, which presents the lowest barrier for process (i) (see Fig. 3 and Table II). In the exchange at $T = 548$ K, a two-step mechanism is clear: the atom of the step comes out as in process (i); a dimer is formed for 3 ps and finally the original adatom is incorporated in the step. In the two exchanges occurring at $T = 592$ K, the two parts of the mechanism cannot be clearly separated, as the whole events occur within 0.5 ps; this fact may give an indication of a concerted motion. However, the frequency of the exchanges is on the scale of ns even at the highest temperature, as predicted in Sec. III on the basis of the barriers related to the two-step mechanism; therefore that mechanism seems to give a reasonable description.

The dependence of r_j on the inverse temperature follows the usual Arrhenius behavior:

$$r_j = r_{j0} \exp\left(-\frac{E_a}{k_B T}\right); \tag{8}$$

the prefactor r_{j0} and the activation energy E_a can be extracted from the results of the simulations. This has been done for both steps in Ag and for step B in Au; as for step A in gold, the statistics is really poor except for two temperatures and the extraction of the parameters from an Arrhenius plot is not meaningful. The three Arrhenius plots are reported in Figs. 8–10. The parameters extracted from the plots are $r_{j0} = 0.8\ \text{ps}^{-1}$ and $E_a = 0.17$ eV for step B in gold, $r_{j0} = 1.9\ \text{ps}^{-1}$ and $E_a = 0.22$ eV for step A in silver, and $r_{j0} = 1.8\ \text{ps}^{-1}$ and $E_a = 0.23$ eV for step B in silver. In any case, the activation barrier E_a is significantly lower than the static potential barrier (see Table II for a comparison), with the standard deviations on the values of E_a being between 0.02 and 0.03 eV; the prefactors are of the order of magnitude of typical vibration frequencies, in qualitative agreement with TST.

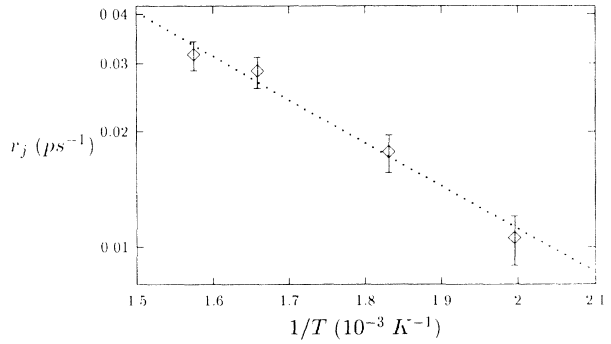

FIG. 9. Arrhenius plot of the jump rate r_j concerning diffusion along step A in Ag. The error bars correspond to the standard deviation.

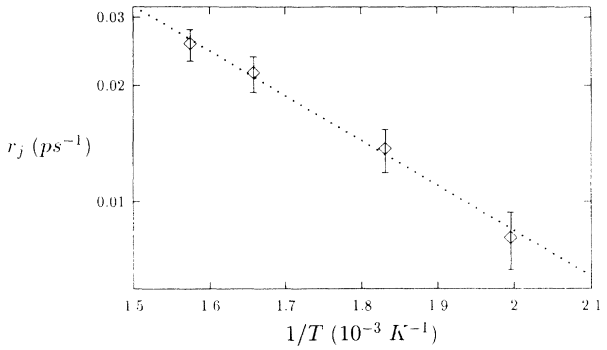

FIG. 10. Arrhenius plot of the jump rate r_j concerning diffusion along step B in Ag. The error bars correspond to the standard deviation.

With the exception of step A in Au, at the temperatures of the simulations, the diffusion along the steps is not much slower than the diffusion on the flat surface. In our case, the MD simulations give a surface diffusion coefficient D_S between 1 and $3 \times 10^{-5}\ \text{cm}^2\,\text{s}^{-1}$ for Au in the range 400–600 K and between 5 and $8 \times 10^{-5}\ \text{cm}^2\,\text{s}^{-1}$ for Ag in the range 500–650 K.

B. Disordering of the steps

Many of the events represented in Fig. 3 lead to the disordering of the steps. As the temperature increases, their characteristic time scales approach the typical time scales of the jumping of the adatom, perturbing its diffusive motion.

In Au, one of those events happens even at 498 K; at this temperature the process (g) of Fig. 3 takes place once and a stable dimer is formed which resists until the end of the simulation (for about 70 ps). More events take place at 548 and 592 K, in particular along step A. For instance, let us consider the highest temperature. Along step A event (d) happens seven times; in six cases the

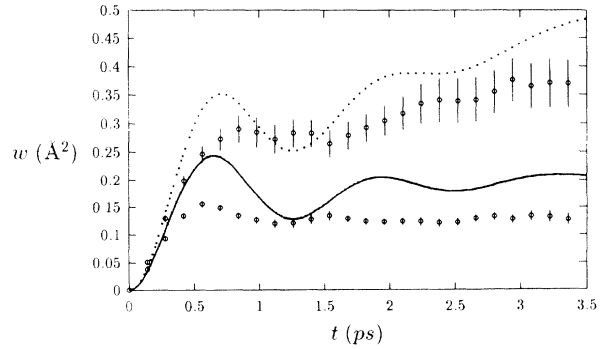

FIG. 11. Mean-square displacement w as a function of time for diffusion along step A in Au. The dots with error bars are the simulation results at 452 and 592 K (lower and upper series, respectively). The full and the dotted lines show the FPE results at the same temperatures.

atom is reincorporated in the step as in process (e) after an existence in the channel of a few ps; only in one case does the atom diffuse in the channel [process (f)] and this proportion agrees well with the estimate given in Sec. III. Concerning the formation of dimers, process (g) happens one time, forming a dimer for 45 ps; process (i) happens three times of which two are related to the exchanges and the third is ended by process (j) in 8 ps. In one simulation the adatom leaves the channel and diffuses onto the lower terrace. Along step B, only two events happen. A dimer as in process (i) is formed, resisting for 6 ps. Moreover, an atom of the step comes out as in (d) and then diffuses along the step. In fact, the discussion in Sec. III has shown that the situation is reversed in the case of step B, and once the atom is in the channel it has a larger probability of diffusing than of coming back and refilling the vacancy.

In Ag, fewer events happen. The most common in both steps is process (g) (six times in total), which is usually terminated by process (h) within 10 ps except for one case along step A in which the whole dimer performs a jump leaving the vacancy behind.

C. Comparison with the FPE results

In order to estimate the dynamical coupling (essentially the microscopic friction) between the adatom and the substrate, TST is not sufficient and more sophisticated rate theories should be used. In the following we will describe the motion of the adatom along the step as the motion of a classical particle in a 1D periodic potential; the particle can exchange energy with the thermal bath by means of a stochastic force $m\Gamma(t)$ and of the friction η. Models of this kind have been widely employed in the field of surface diffusion with rather good results[30,32,33] and they are not simply phenomenological, as they can be derived from more fundamental models.[4,33,35] Assuming $\Gamma(t)$ to be δ correlated, the stochastic differential equation for the motion of the adatom assumes the well-known Langevin form[52]

$$m\frac{dv}{dt} = -m\eta v + m\Gamma(t) + F(x), \tag{9}$$

where x is the coordinate along the step, v is the velocity of the adatom, and $F(x) = -U'(x)$, with $U(x)$ 1D potential. The potential $U(x)$ is known as the adiabatic potential[33,35,4] and actually it is a free energy and depends on temperature; for instance, for diffusion on the flat surface of a Lennard-Jones crystal, the amplitude of the adiabatic potential decreases linearly with T.[33] This form of the Langevin equation is completely equivalent to the FPE,[52] which will be actually solved in the following. $U(x)$ is taken as a simple cosine:

$$U(x) = -\frac{E_b}{2}\cos\left(\frac{2\pi x}{a}\right). \tag{10}$$

A priori, the barrier E_b is taken as a parameter to be fitted on the data of the simulation; it will be interesting to see whether the good values for E_b will agree either with the activation barriers E_a (as extracted from the Arrhenius plots) or with the static potential barriers, as calculated by the quenching procedure. This model can describe different diffusion mechanisms:[36] jump diffusion is recovered in the high-barrier limit, with the possibility of long jumps depending on the friction;[50,51] a quasifree diffusion is obtained at low barriers.[36]

We remark that this model implies some simplifying assumptions; for instance, a 1D model is appropriate in the case of B steps, where the diffusion path is really a straight line. In fact, if the minima and the saddle points of the three-dimensional adiabatic potential acting on the diffusing particle are on a straight line, the diffusive motion can be described as a one-dimensional motion along the diffusion path in a renormalized potential.[4,35] We have shown that in A steps the minima and the saddle points are not even approximately on a straight line and therefore the application of a 1D model is more questionable, especially in Au. Furthermore, the assumption of a δ-correlated stochastic force is justified if the typical vibrational motion of the adatom is slower than that of the other atoms of the surface;[33] this may be the case, as the mass of the adatom is the same as the other surface atoms and the binding of the adatom is weaker.

If the two parameters of the model (E_b and η) are constant in the temperature range of the simulations, they can be extracted from the simulation results at one temperature and used for predicting the results at the other temperatures. First of all, for each metal, the highest simulation temperature for the B step is considered; we have chosen the highest temperature in order to have the data with the best statistics and B steps as the 1D model is surely appropriate for them. At this temperature, the FPE is numerically solved; the jump rate r_j and the jump-length probability distribution are calculated by the Fourier analysis of the frequency width of the quasielastic peak of the dynamic structure factor,[50] as functions of E_b and η. The two parameters are then adjusted to reproduce the right jump rate r_j and the right proportion of long jumps, as results from the MD simulation; then, having fixed the two parameters, r_j and the jump-length probabilities are calculated at the other temperatures. As for step A, the friction η is not readjusted; therefore it is taken to be the same as in step B. Only the barrier E_b is fitted to reproduce r_j at the highest temperature. The results are summarized in Tables V and VI.

In any case, the barriers E_b are lower than the static potential barriers, by about $20-25\,\%$; the relaxations of the barriers with respect to 0 K show no significant differences between the steps and between the metals. When the E_b can be compared with the Arrhenius barriers E_a, i.e., in the case of both steps in silver and of step B in gold, they are in almost perfect agreement. If the E_b were assumed to be equal to the static barriers, the fitting of the friction η to reproduce r_j as in the simulations would not be possible at all. We may conclude that the free-energy barrier for diffusion at high temperatures is really different from the static potential barrier; reliable estimates are given by the Arrhenius plots.

The friction η is always in the intermediate range,

TABLE V. Results of the FPE about gold; E_b is the barrier of the 1D periodic potential, η is the friction, T is the temperature, and r_j is the jump rate as calculated by means of the FPE; P_1, P_2, and P_3 are the probabilities of single, double, and triple jumps.

Step	E_b (eV)	η (ps^{-1})	T (K)	r_j (ps^{-1})	P_1	P_2	P_3
A	0.26	1.7	452	1.7×10^{-3}	0.957	0.041	0.002
A	0.26	1.7	498	3.1×10^{-3}	0.947	0.050	0.003
A	0.26	1.7	548	5.2×10^{-3}	0.936	0.060	0.004
A	0.26	1.7	592	7.8×10^{-3}	0.926	0.068	0.006
B	0.18	1.7	452	1.0×10^{-2}	0.941	0.056	0.003
B	0.18	1.7	498	1.6×10^{-2}	0.931	0.064	0.005
B	0.18	1.7	548	2.3×10^{-2}	0.921	0.073	0.006
B	0.18	1.7	592	2.9×10^{-2}	0.913	0.079	0.008

which characterizes the turnover region in the rate curves.[47,50] In fact, the normalized friction γ,[50] defined as $\gamma = \eta\tau_{\rm th}/(2\pi)$, is about $0.5 - 0.6$, with small differences between the two metals (γ is slightly higher in Ag). This indicates that the velocity correlation time τ_v, related to the friction simply by $\tau_v \sim \eta^{-1}$, is smaller than $\tau_{\rm th}$, but it is not completely negligible. In this condition long jumps are possible but with small probabilities,[50,36] as inertial trajectories are likely to be damped within the first cell. The turnover region is the only one in which TST is a reasonable approximation; this explains the fact that the prefactors in the Arrhenius plots are of the order of magnitude of typical vibration frequencies. In the low- or high-friction regimes the prefactors should have been much smaller.[34,50]

The agreement between the values of r_j given by the simulations and those predicted by the one-dimensional FPE is remarkable. Notice that only the values at the highest temperature are fitted and the friction is not readjusted for step A. Some discrepancies are evident only for step A in Au, especially for the two lowest temperatures. However, at these temperatures the statistics furnished by the simulations is really poor.

The FPE predicts that the probabilty of long jumps will be always of the order of few percents. Almost all long jumps should be double jumps, as the probability of longer jumps is less than 1% in any case. This well agrees with the simulations, where only one triple jump has been observed. Moreover, the FPE predicts some lowering of the long-jump probabilities with decreasing temperature, even in the case of constant friction and adiabatic potential amplitude (as assumed in our case); however, this decrease should not be very strong in the temperature range considered. In step B of Au, the predicted double-jump probabilities are in good agreement with the simulation at 548 and 452 K; at 498 K the statistics should be improved to draw a conclusion. In silver, it seems that the decrease of the double-jump probability at low temperature is somewhat stronger than predicted by the FPE with temperature-independent friction; however, the FPE is in good agreement with the simulations except for the lowest temperature, where no long jumps are seen along both steps. Finally, we consider step A in Au, where long jumps have never been observed; as the FPE predicts a percentage of double jumps comparable to that for step B, we may infer that the topology of the diffusion path, being far from a straight line, causes the stopping of inertial flights.

Therefore we can conclude that the 1D FPE, together with the assumptions concerning the shape of the potential and the friction, gives a very good description of the long-time diffusive dynamics of the adatoms along the steps, with the only exception of step A in Au. In particular, the assumption of an amplitude of the adiabatic potential, which is constant within the temperature range of the simulation, is consistent with all the results in Ag and with those for step B in gold. This fact is not surprising; for instance, for step A in gold the total variation of the amplitude of the adiabatic potential in the range 0–600 K is of 0.04 eV; if a linear decrease of the amplitude with T is assumed,[33] the decrease in the range 450–600 K should be only 0.01 eV. As for step A in Au,

TABLE VI. Results of the FPE about silver; E_b is the barrier of the 1D periodic potential, η is the friction, T is the temperature, and r_j is the jump rate as calculated by means of the FPE; P_1, P_2, and P_3 are the probabilities of single, double, and triple jumps.

Step	E_b (eV)	η (ps^{-1})	T (K)	r_j (ps^{-1})	P_1	P_2	P_3
A	0.21	2.6	501	1.2×10^{-2}	0.952	0.046	0.002
A	0.21	2.6	546	1.7×10^{-2}	0.944	0.053	0.003
A	0.21	2.6	603	2.6×10^{-2}	0.935	0.061	0.004
A	0.21	2.6	635	3.2×10^{-2}	0.930	0.065	0.005
B	0.22	2.6	501	0.9×10^{-2}	0.953	0.045	0.002
B	0.22	2.6	546	1.5×10^{-2}	0.945	0.052	0.003
B	0.22	2.6	603	2.1×10^{-2}	0.936	0.060	0.004
B	0.22	2.6	635	2.6×10^{-2}	0.931	0.064	0.005

there is some indication of a steeper variation of the rate, which may be explained by a non-negligible variation of the potential amplitude in the temperature range of the simulations.

By solving the FPE, the short-time dynamics of the diffusing particle can be described as well; for instance, the mean-square displacement w as a function of time can be numerically calculated[36] by a proper integration of the dynamic structure factor. $w(t)$ is a severe test for the assumptions in the model, as its behavior at short times is sensitive to the details of the potential shape. The results of both simulations and numerical calculations are shown in Figs. 11–14, where for each step and each metal the highest and the lowest simulation temperatures are considered.

In general, w starts as a parabola (related to the inertial motion at very short times) and at long times it recovers linearity, i.e., the diffusive behavior. Between the two regimes there is a knee which is more pronounced at low temperatures; in fact, while the curvature of the initial parabola increases linearly with T (as the square of the thermal velocity), the slope of the asymptotic straight line (which is simply the double of the diffusion coefficient) is proportional to $\exp(-E_b/k_BT)$ and thus varies much more rapidly with temperature. At the times immediately following the knee, some oscillations (no more than two) can be seen. In fact, as the velocity correlation time is smaller than but of the same order as the small-oscillation period (something more and something less than 1 ps for Au and Ag, respectively), there is a certain probability of having some correlated oscillations.

The agreement between the simulations and the FPE results is very good in the case of B steps (see Figs. 12 and 14) at low and high temperatures for both gold and silver. In the case of silver, the oscillations have essentially the same period in the simulation and in the calculations; this indicates that the shape of the effective one-dimensional potential is really similar to a cosine. In the case of gold, the cosine shape gives an oscillation period which is larger by about 0.2 – 0.3 ps than the real one. In this case the cosine is less appropriate; a potential with a slightly narrower well should be better. However, for simplicity, we have not tried to fit the shape of the potential, as the agreement is sufficient with the simple cosine.

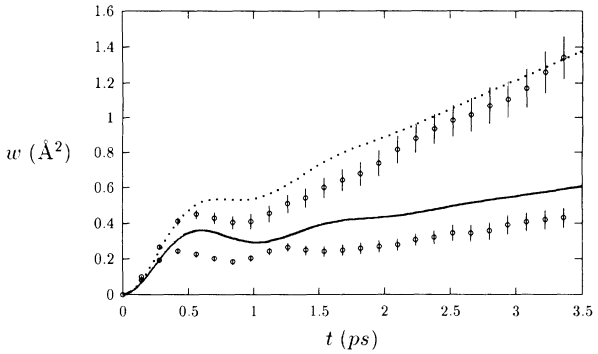

FIG. 13. Mean-square displacement w as a function of time for diffusion along step A in Ag. The dots with error bars are the simulation results at 501 and 635 K (lower and upper series, respectively). The full and the dotted lines show the FPE results at the same temperatures.

The FPE results are not as good in the case of A steps, especially for Au (Fig. 11) (as usual), where the FPE predicts large oscillations which are not present in the simulations. In the case of adatom diffusion on a flat crystal surface, it has been shown that the friction should be position dependent and precisely stronger at the well bottom than at the saddle point.[33] For a given average friction, such a dependence should not change drastically the diffusion coefficient,[31] but it should suppress correlated oscillations at the well bottom. This may explain why the FPE with position-independent friction has the tendency to enhance oscillations in $w(t)$. In Ag, the agreement is good at high temperature and qualitative at low temperature (see Fig. 13); the oscillations are essentially of the same evidence both in the simulations and in the calculations. These results show once again that the one-dimensional model is really oversimplified in the case of the step A in gold and is reasonable for the corresponding step in silver.

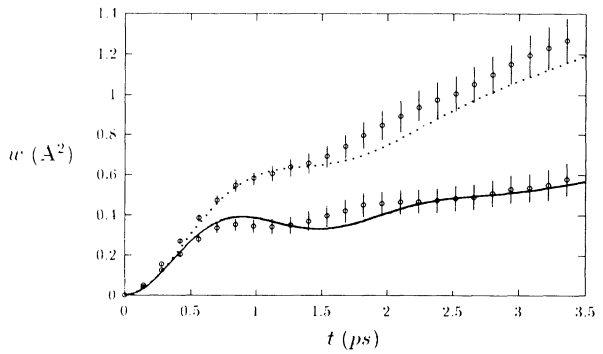

FIG. 12. Mean-square displacement w as a function of time for diffusion along step B in Au. The dots with error bars are the simulation results at 452 and 592 K (lower and upper series, respectively). The full and the dotted lines show the FPE results at the same temperatures.

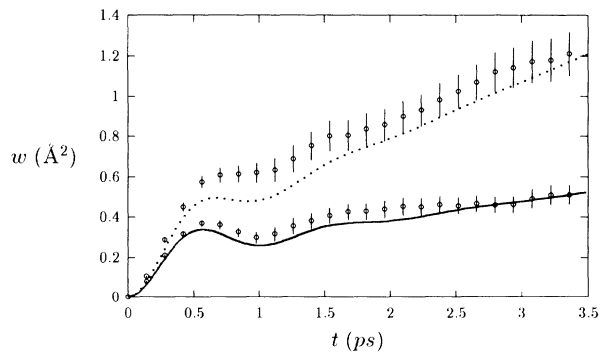

FIG. 14. Mean-square displacement w as a function of time for diffusion along step B in Ag. The dots with error bars are the simulation results at 501 and 635 K (lower and upper series, respectively). The full and the dotted lines show the FPE results at the same temperatures.

V. CONCLUSIONS

In this paper we have performed a molecular-dynamics simulations of diffusion along the two close-packed steps (step A and step B; see Fig. 1) on the (111) surfaces of gold and silver, by using many-body potentials derived within the second-moment approximation to the tight-binding model.[27,37,38] The tight-binding MD simulations predict that gold and silver should behave in a very different way: in gold, diffusion is much faster along step B; in silver, the opposite happens, but the difference between the two steps is less pronounced. In any case, no crossover in the Arrhenius plots of r_j or D is observed; at any temperature, the diffusion is faster along the step which has a lower energy barrier at 0 K. The results of the simulations are consistent with a dynamical lowering of the activation barrier with respect to the static potential barrier of about 20% in the temperature range between 450 and 600 K. This lowering decreases the difference between the diffusion barriers along the two steps, but it does not lead to the inversion in the magnitude even in the case of silver, where the 0 K barriers differ only by 0.04 eV. A slow diffusion along a step should lead to the accumulation of atoms and to a fast growth perpendicular to the step itself, which tends to disappear.[24] From the results of our simulations it should follow that the growth shape of 2D islands on the gold (111) surface is sharply triangular at any temperature with triangles bounded by B steps; in silver, at low temperature, the triangles should be bounded by A steps, but with increasing temperature there might be a change towards an hexagonal shape, as the difference between the diffusion coefficients becomes rather small. According to our simulations, no inversion of the growth-speed anisotropy [which has been found in Pt(111) (Ref. 24)] can be predicted on the basis of the mobility along straight steps, both for gold and for silver.

As the diffusion along steps is expected to be essentially one dimensional, the results of the simulations have been compared to those of a model based on the Fokker-Planck equation in a 1D periodic potential. The agreement of the FPE with the simulation is remarkably good, in the case of B steps in both metals: the theory is able to predict the values of the rate and the correct proportion of long jumps (which is of the order of some percents); moreover, the behavior of the mean-square displacement as a function of time is almost perfectly reproduced both at low and at high temperatures. Along those steps, the diffusion path is really a straight line and a 1D model is essentially correct. In the case of A steps, the agreement is satisfactory for silver, especially for what concerns the rate at any temperature, the proportion of long jumps and the mean-square displacement at high temperature. For step A in gold, the agreement is only qualitative. But in the latter case, the agreement is not expected to be good, as the diffusion path is rather different from a straight line (see Fig. 4) and the application of a 1D model may be questionable.

ACKNOWLEDGMENTS

The authors are grateful to B. Legrand for a careful reading of the manuscript. The CRMC2 is also associated with the Universities of Aix-Marseille II and III.

* Present address: Dipartimento di Fisica dell'Università di Genova, Via Dodecaneso 33, 16146 Genova, Italy.

[1] G. Ehrlich and K. Stolt, Annu. Rev. Phys. Chem. **31**, 603 (1980).
[2] T.T. Tsong, Rep. Prog. Phys. **51**, 759 (1988).
[3] R. Gomer, Rep. Prog. Phys. **53**, 917 (1990).
[4] T. Ala-Nissila and S.C. Ying, Prog. Surf. Sci. **39**, 227 (1992).
[5] S.J. Lombardo and A.T. Bell, Surf. Sci. Rep. **13**, 1 (1991).
[6] G. Wahnström, in *Interactions of Atoms and Molecules with Solid Surfaces*, edited by V. Bortolani, N.H. March, and M.P. Tosi (Plenum, New York, 1990).
[7] G. Ehrlich, Surf. Sci. **246**, 1 (1991); M. Lovisa and G. Ehrlich, J. Phys. (Paris) Colloq. **50**, C8-279 (1989).
[8] E. Ganz, S.K. Theiss, I.S. Hwang, and J. Golovchenko, Phys. Rev. Lett. **68**, 1567 (1992).
[9] J.W.M. Frenken, B.J. Hinch, J.P. Toennies, and Ch. Wöll, Phys. Rev. B **41**, 938 (1990).
[10] J. Ellis and J.P. Toennies, Phys. Rev. Lett. **70**, 2118 (1993).
[11] K.D. Dobbs and D.J. Doren, J. Chem. Phys. **97**, 3722 (1992).
[12] D.E. Sanders and A.E. DePristo, Surf. Sci. **264**, L169 (1992).
[13] C.L. Chen and T.T. Tsong, J. Vac. Sci. Technol. A **10**, 2178 (1992); S.C. Wang and G. Ehrlich, Phys. Rev. Lett. **62**, 2297 (1989); G. Ayrault and G. Ehrlich, J. Chem. Phys. **60**, 281 (1974); C.L. Kellogg and P.J. Feibelman, Phys. Rev. Lett. **64**, 3143 (1990); J.D. Wrigley and G. Ehrlich, *ibid.* **44**, 661 (1980).
[14] G. De Lorenzi, G. Jacucci, and V. Pontikis, Surf. Sci. **116**, 391 (1982).
[15] J.E. Black and Zeng-Ju Tian, Phys. Rev. Lett. **71**, 2445 (1993).
[16] K.D. Shiang, C.M. Wei, and T.T. Tsong, Surf. Sci. **301**, 137 (1994).
[17] P. Stolze and J.K. Norskov, Phys. Rev. B **48**, 5607 (1993).
[18] R. Stumpf and M. Scheffler, Phys. Rev. Lett. **72**, 254 (1994).
[19] R. Wang and K.A. Fichthorn, Surf. Sci. **301**, 253 (1994).
[20] D.E. Sanders, D.M. Halstead, and A.E. DePristo, J. Vac. Sci. Technol. A **10**, 1986 (1992).
[21] S.C. Wang and G. Ehrlich, Phys. Rev. Lett. **67**, 2509 (1991).
[22] R.C. Nelson, T.L. Einstein, S.V. Khare, and P.J. Rous, Surf. Sci. **295**, 462 (1993).
[23] H.-J. Ernst, F. Fabre, and J. Lapujoulade, Phys. Rev. Lett. **69**, 458 (1992).
[24] T. Michely, M. Hohage, M. Bott, and G. Comsa, Phys. Rev. Lett. **70**, 3943 (1993).
[25] T. Michely, K.H. Besocke, and G. Comsa, Surf. Sci. **230**,

L135 (1990).
[26] J.C. Heyraud and J.J. Métois, Surf. Sci. **100**, 519 (1980), Y. Tanishiro, H. Kanamori, K. Takayanagi, K. Yagi, and G. Honjo, Surf. Sci. **111**, 395 (1981); U. Harten, A.M. Lahee, J.P. Toennies, and Ch. Wöll, Phys. Rev. Lett. **54**, 2619 (1985).
[27] V. Rosato, M. Guillopé, and B. Legrand, Philos. Mag. A **59**, 321 (1989).
[28] C. Mottet, G. Tréglia, and B. Legrand, Phys. Rev. B **46**, 16 018 (1992).
[29] K.D. Shiang and T.T. Tsong, Phys. Rev. B **49**, 7670 (1994).
[30] J.R. Banavar, M.H. Cohen, and R. Gomer, Surf. Sci. **107**, 113 (1981); V.P. Zhdanov, *ibid.* **214**, 289 (1989); R. Ferrando, R. Spadacini, and G.E. Tommei, *ibid.* **251/252**, 773 (1991); E. Pollak, J. Bader, B.J. Berne, and P. Talkner, Phys. Rev. Lett. **70**, 3299 (1993).
[31] R. Ferrando, R. Spadacini, and G.E. Tommei, Surf. Sci. **265**, 273 (1992).
[32] R. Ferrando, R. Spadacini, and G.E. Tommei, Phys. Rev. B **45**, 444 (1992).
[33] G. Wahnström, J. Chem. Phys. **84**, 5931 (1986); Surf. Sci. **159**, 311 (1985); Phys. Rev. B **33**, 1020 (1986).
[34] L.Y. Chen and S.C. Ying, Phys. Rev. Lett. **71**, 4361 (1993).
[35] S.C. Ying, Phys. Rev. B **41**, 7068 (1990).
[36] R. Ferrando, R. Spadacini, G.E. Tommei, and G. Caratti, Physica A **195**, 506 (1993).
[37] J. Friedel, in *The Physics of Metals*, edited by J.M. Ziman (Cambridge University Press, Cambridge, 1969), p. 340.
[38] F. Ducastelle, J. Phys. (Paris) **31**, 1055 (1970).
[39] D. Tomanek, A.A. Aligia, and C.A. Balseiro, Phys. Rev. B **32**, 5051 (1985).
[40] R.P. Gupta, Phys. Rev. B **23**, 6265 (1981).
[41] M. Guillopé and B. Legrand, Surf. Sci. **215**, 577 (1989); B. Legrand, M. Guillopé, J.S. Luo, and G. Tréglia, Vacuum **41**, 311 (1990).
[42] M.P. Allen and D.J. Tildesley, *Computer Simulation of Liquids* (Clarendon, Oxford, 1987).
[43] C.H. Bennett, in *Diffusion in Solids, Recent Developments*, edited by A.S. Nowick and J.J. Burton (Academic, New York, 1975), p. 73.
[44] S.C. Wang and G. Ehrlich, Surf.Sci. **239**, 301 (1990).
[45] S.C. Wang and G. Ehrlich, Phys. Rev. Lett. **70**, 41 (1993).
[46] J. Norskov (unpublished).
[47] P. Hänngi, P. Talkner, and M. Borkovec, Rev. Mod. Phys. **62**, 251 (1990), and references therein.
[48] D.W. Basset and P.R. Webber, Surf. Sci. **70**, 520 (1978).
[49] P.J. Feibelman, Phys. Rev. Lett. **65**, 729 (1990).
[50] R. Ferrando, R. Spadacini, and G.E. Tommei, Phys. Rev. E **48**, 2437 (1993); R. Ferrando, R. Spadacini, G.E. Tommei, and G. Caratti, Surf. Sci. **311**, 411 (1994).
[51] V.I. Melnikov, Phys. Rep. **209**, 1 (1991).
[52] H. Risken, *The Fokker-Planck Equation* (Springer, Berlin, 1989).

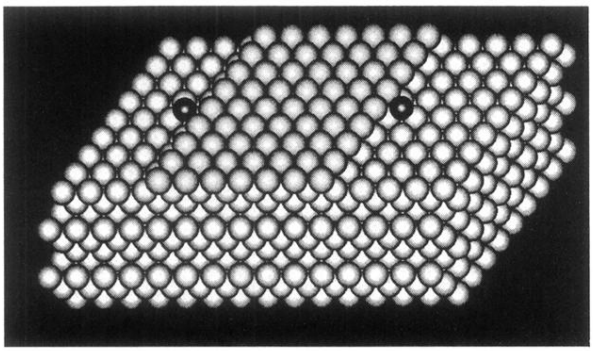

FIG. 2. The slab used in the simulations. The terrace on the topmost layer is bounded by an A step on the left and a B step on the right. In both channels along the steps there is an adatom.